

## LITERATURE CITED

1. L. I. Sedov, *Prikl. Mat. Mekh.*, **32**, No. 6 (1968).
2. Long-sun Tong, *Boiling Heat Transfer and Two-Phase Flow*, Wiley, New York (1965).
3. V. A. Barilovich, V. V. Batuev, V. A. Zysin, T. N. Parfenova, and S. G. Platonova, in: *Power Machinery Construction. Proceedings of the Leningrad Polytechnic Institute [in Russian]*, No. 316, Mashinostroenie, Leningrad (1970).
4. P. P. Vegener and L. M. Mak, in: *Problems of Mechanics [in Russian]*, No. 4, Moscow (1961).
5. L. S. Pontryagin, *Ordinary Differential Equations*, Addison-Wesley, Reading (1962).
6. L. A. Vulis, P. L. Gusika, and G. V. Zhizhin, *Zh. Prikl. Mekh. Tekh. Fiz.*, No. 5, 143 (1972).
7. H. Poincaré, *Curves Determined by Differential Equations [Russian translation]*, GITTL, Moscow-Leningrad (1947).
8. L. A. Vulis, *Thermodynamics of Gas Flows [in Russian]*, Gosénergoizdat, Moscow (1950).
9. S. J. Reed, *J. Chem. Phys.*, No. 20 (1952).
10. R. D. Buhler, *Condensation of Air Components in Hypersonic Wind Tunnels*, California Institute of Technology, Pasadena (1952).

## ASYMMETRY OF THERMOGRAVITATIONAL CONVECTION

P. F. Zavgorodnii, I. L. Povkh,  
G. M. Sevost'yanov, and N. S. Sidel'nikova

UDC 536.252:532.781

The nature and intensity of convective motion in a rectangular region with moving boundaries of the solidification front are studied by the finite-difference method.

Thermal convection in regions with moving boundaries of the solidification front, its nature, and intensity have an important effect on heat and mass transfer in the liquid phase, on the redistribution of an admixture in the solid crust, and on the macrostructure of the finished casting. The three-dimensional problem of unsteady thermal convection in a rectangular prism was formulated and solved in [1]. The plane case of thermal convection was analyzed in [2] and that for a cylindrical region, in [3]. The considerable divergence in the calculated results and in some cases the contradiction of the conclusions indicate the necessity of further study of this problem with the aim of clarifying the determining factors of the process of thermal convection.

A region of rectangular cross section, semiinfinite along the coordinate  $\eta_2$ , was chosen for study in the present report. The region is filled with a stationary homogeneous melt with an initial temperature  $T_0$  higher than its crystallization temperature.

Proceeding from the assumption that the vertical axis  $O\eta_3$  is the axis of symmetry of the convective streams, one of the halves of the region under consideration is represented in Fig. 1. The dimensions in the diagram are relative, with the horizontal width being taken as the characteristic size, so that  $l_1 = 1$ .

At a time  $\tau > 0$  the temperature of the boundaries of the region is abruptly reduced to the crystallization temperature, as a result of which the solid phase is formed at the periphery. The solidification front is assumed to be plane. The dimensions of the liquid phase along the coordinates  $\eta_1$  and  $\eta_3$  and the thickness of the top crust are assumed to be known functions of time:

$$\varepsilon_1 = 1 - k_1 \sqrt{Fo}; \quad \varepsilon_3 = l_3 - k_2 \sqrt{Fo}, \quad H = k_3 \sqrt{Fo}, \quad (1)$$

where  $k_1$ ,  $k_2$ , and  $k_3$  are solidification coefficients.

In the Boussinesq approximation the initial system of equations in dimensionless vector form is written

Donets State University. Translated from *Inzhenerno-Fizicheskii Zhurnal*, Vol. 32, No. 1, pp. 102-108, January, 1977. Original article submitted April 21, 1975.

*This material is protected by copyright registered in the name of Plenum Publishing Corporation, 227 West 17th Street, New York, N.Y. 10011. No part of this publication may be reproduced, stored in a retrieval system, or transmitted, in any form or by any means, electronic, mechanical, photocopying, microfilming, recording or otherwise, without written permission of the publisher. A copy of this article is available from the publisher for \$7.50.*

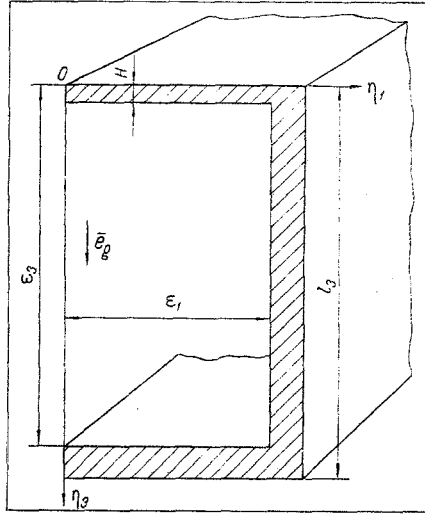


Fig. 1. Diagram of the crystallizing region.

$$\frac{1}{\text{Pr}} \frac{\partial \bar{V}}{\partial \text{Fo}} + (\bar{V} \nabla) \bar{V} = -\nabla \pi + \nabla \bar{V} + \bar{e}_g \text{Gr} \Theta, \quad (2)$$

$$\frac{\partial \Theta}{\partial \text{Fo}} + \text{Pr} (\bar{V} \nabla) \Theta = \nabla \Theta, \quad (3)$$

$$\nabla \bar{V} = 0. \quad (4)$$

The following boundary conditions are used for the solution of system (2)-(4):

$$\Theta = 1, \quad V_1 = V_3 = 0 \quad \text{at} \quad \text{Fo} = 0;$$

$$\frac{\partial \Theta}{\partial \eta_1} = \frac{\partial V_3}{\partial \eta_1} = V_1 = 0 \quad \text{at} \quad \eta_1 = 0; \quad (5)$$

$$\Theta = V_1 = V_3 = 0 \quad \text{at} \quad \eta_1 = \epsilon_1, \quad \eta_3 = H, \quad \text{and} \quad \eta_3 = \epsilon_3.$$

Region of variation of the variables:  $0 \leq \eta_1 \leq \epsilon_1$ ;  $0 \leq \eta_3 \leq \epsilon_3$ .

The presence of moving boundaries of the solidification front in the liquid phase considerably complicates the problem and leads to certain additional difficulties caused by the numerical realization of the formulated problem on a computer. In particular, the choice of a coordinate grid in a region which varies with time is difficult when finite-difference systems are used.

Therefore, it is desirable to change to variables in system (2)-(4) such that the region of investigation remains constant during the entire interval of solidification of the liquid zone. For this purpose we introduce the new variables  $\zeta_1$  and  $\zeta_3$  through the equations

$$\zeta_1 = \frac{\eta_1}{\epsilon_1}; \quad \zeta_3 = \frac{\eta_3 - H}{\epsilon_3 - H}.$$

In this case  $0 \leq \zeta_1 \leq 1$  and  $0 \leq \zeta_3 \leq 1$ , i.e., the transition from a rectangular region with moving boundaries to the region of a unit square is accomplished with the variables  $\zeta_1$  and  $\zeta_3$ .

Considering the plane case of the problem, we introduce the stream function  $\Psi$ , which identically satisfies the continuity equation, and the curl of the velocity  $\varphi = \text{curl } \bar{V}$ . After performing the appropriate mathematical transformations, we write system (2)-(4) in the variables  $\zeta_1$  and  $\zeta_3$  in the form

$$\begin{aligned} \frac{\partial \varphi}{\partial \text{Fo}} + \frac{1}{\epsilon_1} \left[ \frac{\text{Pr}}{(\epsilon_3 - H)} \frac{\partial \Psi}{\partial \zeta_3} - \zeta_1 \epsilon_1' \right] \frac{\partial \varphi}{\partial \zeta_1} - \frac{1}{(\epsilon_3 - H)} \left[ \frac{\text{Pr}}{\epsilon_1} \frac{\partial \Psi}{\partial \zeta_1} \right. \\ \left. - \zeta_3 (\epsilon_3' - H') + H' \right] \frac{\partial \varphi}{\partial \zeta_3} = \text{Pr} \Delta_1 \varphi - \frac{\text{Pr} \text{Gr}}{\epsilon_1} \frac{\partial \Theta}{\partial \zeta_1}; \end{aligned} \quad (6)$$

$$\frac{\partial \Theta}{\partial \text{Fo}} + \frac{1}{\epsilon_1} \left[ \frac{\text{Pr}}{(\epsilon_3 - H)} \frac{\partial \Psi}{\partial \zeta_3} - \zeta_1 \epsilon_1' \right] \frac{\partial \Theta}{\partial \zeta_1} - \frac{1}{(\epsilon_3 - H)} \left[ \frac{\text{Pr}}{\epsilon_1} \frac{\partial \Psi}{\partial \zeta_1} - \zeta_3 (\epsilon_3' - H') + H' \right] \frac{\partial \Theta}{\partial \zeta_3} = \Delta_1 \Theta; \quad (7)$$

$$\Delta_1 \Psi = -\varphi. \quad (8)$$

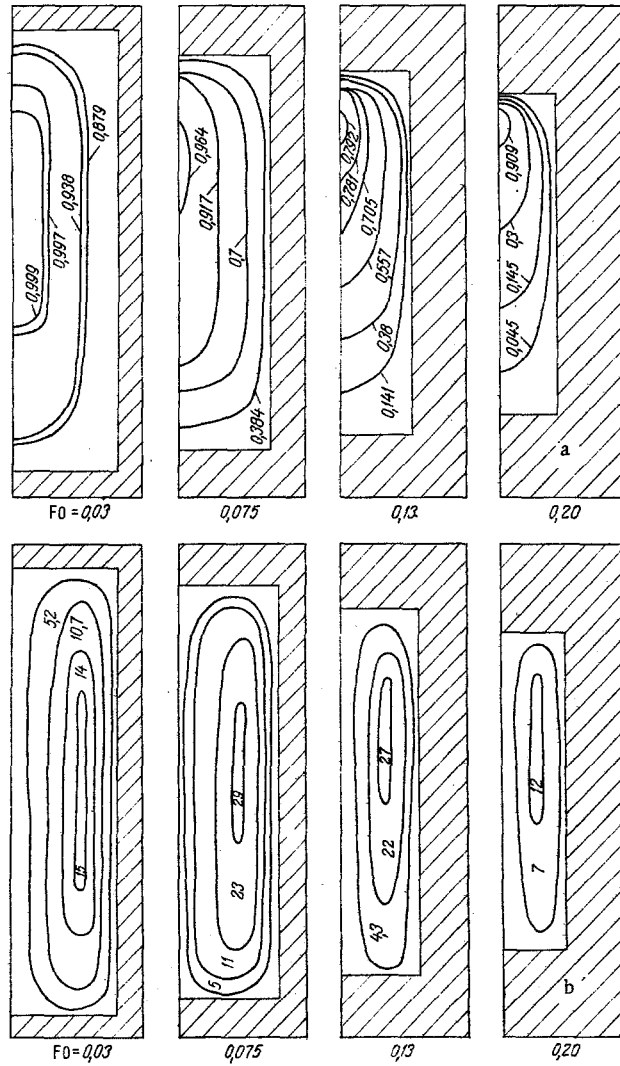


Fig. 2. Isotherms of liquid phase (a) and isolines of stream function (b).  $Gr = 0.22 \cdot 10^5$ ;  $Pr = 0.224$ ;  $L_3 = 4$ .

Here

$$\varepsilon'_1 = -\frac{\partial \varepsilon_1}{\partial Fo}; \quad \varepsilon'_3 = -\frac{\partial \varepsilon_3}{\partial Fo}; \quad H' = \frac{\partial H}{\partial Fo}; \quad \Delta_1 = \frac{1}{\varepsilon_1^2} \frac{\partial^2}{\partial \zeta_1^2} + \frac{1}{(\varepsilon_3 - H)^2} \frac{\partial^2}{\partial \zeta_3^2}.$$

The equations obtained for the curl of the velocity (6) and the temperature (7) have a somewhat complicated character in comparison with the classical equations (in [2], for example). However, such a complication is justified by the fact that the necessity of recalculating the parameters at the nodes of the discrete grid when difference systems are used drops out, since the choice of the variables  $\zeta_1$  and  $\zeta_3$  retains a unit region in the entire interval of investigation and the crystallization front remains at the boundary of the unit region.

To record the equations in finite-difference form we introduce the coordinate grid and time grid through the equations

$$\omega_n = \left\{ \zeta_1 = ih; \quad \zeta_3 = mh; \quad h = \frac{1}{J} = \frac{1}{M}; \quad i, m = 1, 2, \dots, J = M \right\},$$

$$Fo_n = \left\{ Fo = \sum_j \tau_j, \quad \tau = \frac{Ah^2}{4}; \quad 0 < A \leq 1; \quad j = 0, 1, 2, \dots \right\}.$$

A system with separation of the equations with respect to the coordinates  $\zeta_1$  and  $\zeta_3$  was used for the finite-difference approximation of system (6)-(7). The integro-interpolation method [4] is applied to the separated equations on the basis of the requirement of stability of the solution, and the method of variable directions,

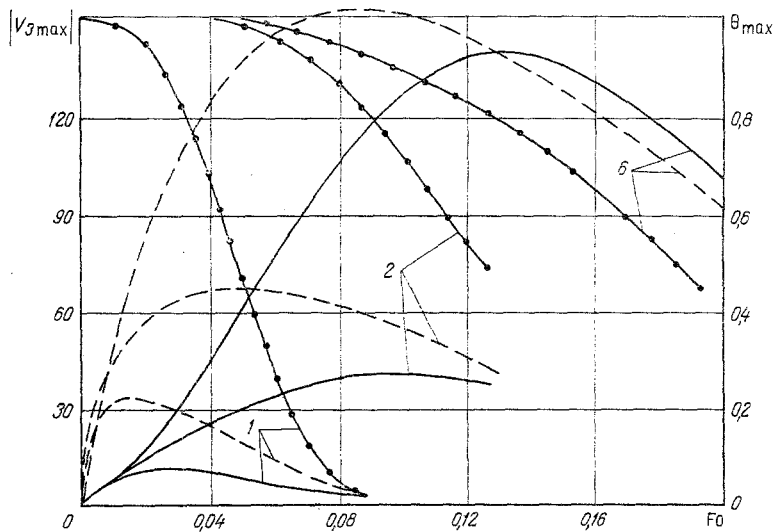


Fig. 3. Dependence of velocity component  $V_3$  in ascending (solid line) and descending flows (dashed line) and of temperature of melt  $\theta$  on time  $Fo$ . Numbers on curves are relative height of cavity;  $Gr = 0.22 \cdot 10^5$ ;  $Pr = 0.224$ .

for which the trial-run equations and coefficients are determined in accordance with the same report, was chosen for the numerical realization on a Dnepr-21 computer.

The calculation procedure was set up as follows. The values of the temperature along the rows of the coordinate grid were calculated in the first time half-step and the values along the columns were calculated in the second. The values of the curl of the velocity and the stream function from the preceding time were used in this case. From the calculated values of the temperature and the initial values of the stream function (for the same two time half-steps) the values of the curl of the velocity were calculated at the grid nodes, from which the values of the stream function were determined by iteration of the Poisson equation (8). After this the time cycle was closed and in the case of complete solidification of the cavity it was ended.

The calculation was conducted on a grid of  $\omega_h = 16 \times 16$  with a time coefficient  $A = 0.3$  and with a fixed Grashof number ( $Gr = 0.22 \cdot 10^5$ ). The solidification coefficients entering into Eqs. (1) were taken as the same and equaled  $k_1 = k_2 = k_3 = 1.25$ , which corresponds to the solidification of a cavity with a characteristic size  $\bar{x}_0 = 0.3$  m in approximately 4 h.

We studied the effect of the relative height of the cavity, the thermophysical properties of the medium, and the initial overheating of the melt on the parameters of the thermal convection.

Figure 2 characterizes the qualitative pattern and dynamics of the development of thermal convection with time for a region with a relative height  $l_3 = 4$ .

In the initial period of solidification upon the instantaneous cooling of the walls of the mold the maximum temperature gradient develops in the region of the melt near the walls (Fig. 2a,  $Fo = 0.03$ ). The melt which is located near the solidifying surface, becoming heavier, descends into the bottom part of the ingot, thereby setting the remaining liquid metal into motion upward along the axis of the cavity. The zone of "descending" flows corresponding to this time is considerably smaller than the zone of "ascending" flows (Fig. 2b,  $Fo = 0.03$ ).

Reorganization of the temperature field of the liquid phase takes place as the thermal convection develops. The hotter layers, carried along by the convective motion, move to the cool walls and, being cooled while moving along them, descend into the bottom part of the ingot. The displacement of the thermal center toward the upper boundary occurs as a result of this (Fig. 2a,  $Fo = 0.075, 0.13, 0.2$ ). The dynamics of the temperature field act in a corresponding way on the velocity field of the liquid region. As the size of the liquid zone decreases, the center of the velocity vortex falls behind the thermal center in moving upward from the side and bottom boundaries so that the zones of ascending and descending flows become equalized (Fig. 2b,  $Fo = 0.075, 0.13, 0.2$ ).

The time distribution of the velocity component  $V_3$  in the ascending and descending flows of melt and of the temperature  $\theta$  for regions with different relative heights  $l_3$  are presented in Fig. 3.

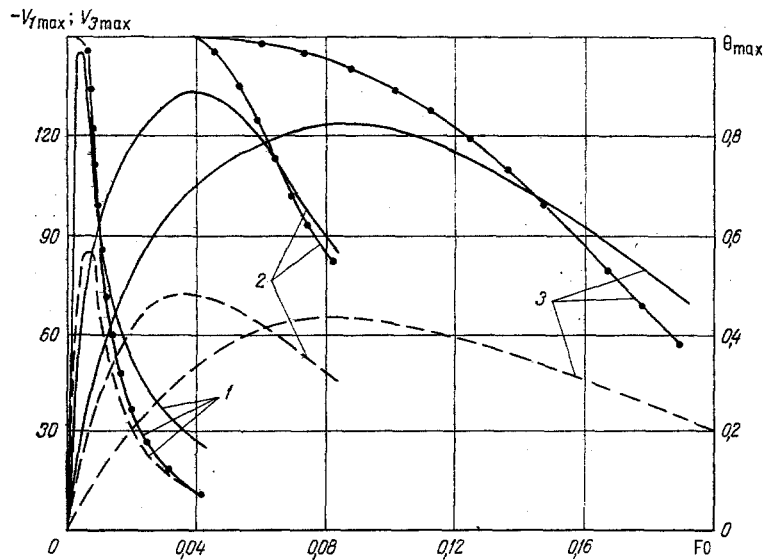


Fig. 4. Effect of Prandtl numbers on unsteadiness of thermogravitational convection. Solid line: velocity component  $V_3$ ; dashed line:  $V_1$ ;  $\odot$ : temperature. Numbers 1, 2, and 3 correspond to Prandtl numbers  $Pr = 8.8, 0.88, \text{ and } 0.224$ ;  $Gr = 0.22 \cdot 10^5$ ;  $l_3 = 4$ .

As the results of the calculation show, regardless of the height of the crystallizing cavity the entire process of thermal convection can be divided into two stages: a stage of acceleration of the melt and one of slowing of the rate of convective motion.

It was noted earlier that a spatial reorganization of the temperature field takes place in the initial period of solidification. This same period is characterized by the rise of the convection velocities. The duration and the maximum value of the velocities in the acceleration stage essentially depend on the relative height  $l_3$  of the cavity. As it increases the intensity of the motion grows with a simultaneous increase in the duration of the acceleration of the melt. It should be noted that the development of the convective motion in the ascending and descending flows does not take place in the same way. While the motion develops almost instantly in the region near the wall, in the axial part of the cavity it develops with a certain delay.

The second stage, more prolonged, generally speaking, is characterized by a decrease in the velocity of the motion. The results of the calculation show that the total duration of the convective motion of the liquid core of the ingot is entirely due to the presence of overheating in the melt (Fig. 3). With the removal of the overheating the intensity of the thermal convection decreases, asymptotically approaching zero.

The effect of the Prandtl number on the nature of the thermal convection is represented in Fig. 4. As the results of the calculation show, variation in the Prandtl number in the range from  $Pr = 0.224$  to  $Pr = 8.8$  has a weak effect on the maximum velocities reached by the melt and acts mainly on the duration of the thermal convection.

An analysis of the initial equations shows that in the case of small Prandtl numbers ( $Pr \ll 1$ ) the equation of heat and mass transfer can be linearized on account of the convective term while the equation of motion can be linearized on account of the convective and viscous terms. In this case the velocities of thermal convection depend on the Rayleigh number, while the mechanism of molecular heat conduction affects the temperature distribution.

For larger Prandtl numbers one can neglect the local time derivative in the equations of motion and heat transfer. A quasisteady regime of thermal convection occurs in this case. The determining criteria of the intensity of the convective motion become the Grashof number and the convective terms, which introduce the essential nonlinearity into the process of thermal convection.

It should be noted that the conclusion drawn in [1] that the regime of thermal convection is "quasisteady" is confirmed by the results of the present work only for large Prandtl numbers.

## NOTATION

$\tau$ , time;  $T$ , temperature of melt;  $T_0$ , initial temperature;  $T_C$ , crystallization temperature of liquid;  $\Psi$ , stream function;  $\bar{\varphi}$ , curl of velocity;  $\nu$ , coefficient of kinematic viscosity;  $a$ , coefficient of thermal diffusivity;  $\bar{x}_0$ , characteristic size of region;  $\bar{e}_g$ , unit vector of  $O\eta_3$  axis;  $l_3$ , relative height of cavity;  $\varepsilon_i$ , relative width of liquid zone ( $i = 1, 3$ );  $\omega_h$ , coordinate grid of region;  $h$ , distance between nodes of coordinate grid;  $A$ , time multiplier;  $T_0 - T_C$ , characteristic temperature difference;  $\bar{p} = \rho \bar{u}_0^2$ , characteristic pressure;  $R = \text{PrGr}$ , Rayleigh number;  $\eta_i = x_i/\bar{x}_0$ , dimensionless coordinates ( $i = 1, 3$ );  $\Theta = (T - T_C)/(T_0 - T_C)$ , dimensionless temperature;  $\pi = p/\bar{p}$ , dimensionless pressure;  $\text{Fo} = \tau/\bar{\tau}$ , dimensionless time (Fourier number);  $\bar{u}_0 = \nu/\bar{x}_0$ , characteristic velocity;  $\bar{\tau} = \bar{x}_0^2/a$ , characteristic time;  $\text{Pr} = \nu/a$ , Prandtl number;  $\text{Gr} = q\beta(T_0 - T_C)\bar{x}_0^3/\nu^2$ , Grashof number.

## LITERATURE CITED

1. É. A. Iodko, P. F. Zavgorodnii, and G. M. Sevost'yanov, *Teplofiz. Vys. Temp.*, **9**, No. 5 (1971).
2. B. I. Vaisman and E. L. Tarunin, in: *Fluid Dynamics [in Russian]*, Uchenye Zapiski No. 293, Perm. Gos. Univ., Perm' (1972).
3. Yu. A. Samoilovich, *Izv. Akad. Nauk UkrSSR, Metally*, No. 2 (1969).
4. A. A. Samarskii, *Introduction to the Theory of Difference Systems [in Russian]*, Nauka, Moscow (1971).

## UNSTEADY CONVECTIVE HEAT TRANSFER IN POTENTIAL FLOW

P. S. Chernyakov

UDC 536.25

Analytical relations are obtained for the unsteady temperature field in potential flow over a flat plate and a cylinder.

Works [1-3] have examined stationary forced convection in potential flow of a liquid over bodies.

The present paper determines the unsteady temperature fields in longitudinal flow over a flat plate with boundary conditions of the first and second kinds, with and without allowance for thermal radiation and motion of the cylinder in the flow with boundary conditions of the first kind. This type of problem is described by the equations for the fluid temperature  $T$ , the velocity potential  $\varphi$ , and the pressure  $p$ :

$$\Delta\varphi = 0, \quad (1)$$

$$\frac{\partial T}{\partial t} + (\text{grad } T, \text{grad } \varphi) = a\Delta T, \quad (2)$$

$$p = p_0 - 0.5\rho(\text{grad } \varphi)^2 - \rho \frac{\partial \varphi}{\partial t} - \rho(\vec{g}, \vec{r}) \quad (3)$$

and initial and boundary conditions on the body surface

$$\frac{\partial \varphi}{\partial n} = U, \quad (4)$$

$$T(\vec{x}, 0) = T_0(\vec{x}), \quad T|_{\vec{x} \in S} = f(\vec{x}_s, t), \quad \lambda \frac{\partial T}{\partial n} \Big|_{\vec{x} \in S} = g(\vec{x}_s, t), \quad (5)$$

$$\lambda \frac{\partial T}{\partial n} \Big|_{\vec{x} \in S} = \sigma(T^4|_{\vec{x} \in S} - T_\infty^4), \quad T|_{\vec{x} \rightarrow \infty} = T_\infty.$$

We assume that the thermophysical properties of the liquid are independent of temperature and pressure and that a similarity transformation  $x_i = \sqrt{a} y_i$  has been derived which results in the coefficient of  $\Delta T$  reducing

---

Institute for Low-Temperature Physics and Engineering of the Academy of Sciences of the Ukrainian SSR, Khar'kov. Translated from *Inzhenerno-Fizicheskii Zhurnal*, Vol. 32, No. 1, pp. 109-115, January, 1977. Original article submitted August 1, 1975.

This material is protected by copyright registered in the name of Plenum Publishing Corporation, 227 West 17th Street, New York, N.Y. 10011. No part of this publication may be reproduced, stored in a retrieval system, or transmitted, in any form or by any means, electronic, mechanical, photocopying, microfilming, recording or otherwise, without written permission of the publisher. A copy of this article is available from the publisher for \$7.50.